PHILOSOPHICAL TRANSACTIONS OF THE ROYAL SOCIETY A MATHEMATICAL, PHYSICAL & ENGINEERING SCIENCES

# Vibration Transmission through Symmetric Resonant Couplings

D. J. Allwright, M. Blakemore, P. R. Brazier-Smith and J. Woodhouse

*Phil. Trans. R. Soc. Lond. A* 1994 **346**, 511-524
doi: 10.1098/rsta.1994.0033

# Vibration transmission through symmetric resonant couplings

By D. J. Allwright[1], M. Blakemore[1], P. R. Brazier-Smith[1] and J. Woodhouse[2]

[1] *SAIC S&E Ltd, Poseidon House, Castle Park, Cambridge CB3 0RD, U.K.*
[2] *Cambridge University Engineering Department, Trumpington Street, Cambridge CB2 1PZ, U.K.*

The transmission of vibration through a symmetric junction is considered. The problem is introduced using a stretched string with a general point attachment, and then a result is derived which encapsulates the important aspects of the transmission behaviour for a wider class of systems. These are systems that consist of two semi-infinite sections of identical, one-dimensional structure having only one propagating wavetype (but any number of evanescent ones), joined through any linear system that satisfies a condition of symmetry. For such systems, it is shown that there will in general be a set of frequencies of perfect transmission and perfect reflection, in a number and pattern which can be described in terms of the behaviour of the junction alone. Representative examples are presented, based on the behaviour of bending beams and thin circular cylinders with attached structures providing wave reflection. The implications of this result are explored for SEA coupling loss factors, and for the interpretation of SEA model predictions when such resonant coupling structures are present.

## 1. Introduction

Fundamental to many problems in noise and vibration control is the understanding of vibration transmission between two systems across a junction of some kind. The level of transmitted vibration, and its distribution in space and frequency, will be governed by the detailed design of the systems and the junction. There are many techniques, theoretical and experimental, for investigating such transmission behaviour. At low frequencies the whole system is likely to exhibit low modal overlap, so that deterministic analysis using idealized theoretical models, finite element analysis, or experimental modal analysis can commonly be used to good effect. Higher in frequency, especially if the modal overlap becomes significant, such treatment becomes very difficult to carry through with acceptable accuracy, and in any case may be of dubious value. One may learn more from an approximate analysis of a stochastic nature, such as statistical room acoustics or statistical energy analysis (SEA) (see, for example, Lyon 1975; Hodges & Woodhouse 1986).

This paper addresses a class of problems that are often encountered in practice, and which present difficulties for both these styles of analysis. It concerns junction structures that have internal degrees of freedom, so that their dynamics must be taken into account in the transmission calculation. If the frequency range of interest is not too high in the modal series of the subsystems coupled through this junction,

*Phil. Trans. R. Soc. Lond.* A (1994) **346**, 511–524
*Printed in Great Britain*

then a deterministic analysis of the whole coupled system may be possible which incorporates the junction behaviour. But at higher frequencies the modal overlap may become high in the subsystems so that a statistical analysis is indicated, but the modal density of the junction structure on its own can still be quite low, so that it may not be appropriate to include it as a third energy-storing subsystem in, for example, a SEA model.

A common starting point for analysing such a system would be to consider the wave reflection/transmission problem in which the two subsystems were regarded as semi-infinite (see, for example, Lyon 1975; Cremer *et al.* 1973). The transmission coefficient across the junction can be calculated as a function of frequency, and if the subsystems are two- or three-dimensional, as a function of angle of incidence at the junction. If a SEA model is required, the coupling loss factor would then be calculated from this transmission coefficient by an averaging procedure (Lyon 1975). This procedure can be applied, at least in principle, to any combination of subsystems and junction. The existence of internal resonances in the junction does not invalidate the approach, but it has significant implications for the interpretation of the results of any modelling. Such internal resonances produce strong frequency dependence of the transmission coefficient, which has immediate consequences for a deterministic study, and rather less obvious ones for the results of a statistical model. The nature and implications of this frequency dependence form the main subject of this study.

## 2. Wave transmission past a point attachment on a stretched string

Consider a stretched string of tension $P$ and line density $m$, having a constraint attached at the point $x = 0$, in the form of a linear system which presents a frequency-dependent (velocity) admittance $Y(\omega)$ to the transverse motion of the string. Assume a transverse displacement field

$$y(x,t) = \mathrm{e}^{-\mathrm{i}\omega t}[\mathrm{e}^{\mathrm{i}kx} + R\,\mathrm{e}^{-\mathrm{i}kx}] \quad (x \leqslant 0), \quad y(x,t) = T\,\mathrm{e}^{-\mathrm{i}\omega t}\,\mathrm{e}^{\mathrm{i}kx} \quad (x \geqslant 0) \tag{2.1}$$

on the string, where $k = \omega(m/P)^{\frac{1}{2}}$. Enforcing the constraint condition at $x = 0$, the transmission coefficient $T$ and reflection coefficient $R$ are readily shown to be

$$T = \frac{2Y}{2Y + Y_0} \quad \text{and} \quad R = \frac{-Y_0}{2Y + Y_0}, \tag{2.2}$$

where $Y_0 = (Pm)^{-\frac{1}{2}}$ is the wave admittance of the string.

We discuss exclusively conservative constraint systems, so that $Y(\omega)$ is purely imaginary at all frequencies. It follows that

$$T/R = -2Y/Y_0 \tag{2.3}$$

is purely imaginary, and that

$$|T|^2 + |R|^2 = \frac{|2Y|^2 + |Y_0|^2}{|2Y + Y_0|^2} = 1 \tag{2.4}$$

as expected.

For any frequency such that $Y \to \infty$, there is perfect transmission of transverse waves past the constraint ($T = 1$, $R = 0$). Conversely, at any frequency such that $Y \to 0$ there is perfect reflection ($T = 0$, $R = -1$). The former case occurs trivially in the absence of any constraint, or at a resonance frequency of the constraining system. The latter case occurs if the constraint takes the form of a fixed point, or at

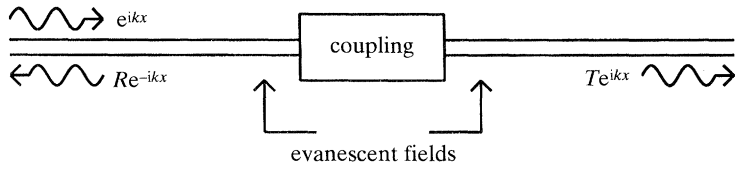


Figure 1. Sketch of two-semi-infinite one-dimensional wave-bearing systems joined by a symmetric coupling.

an antiresonance of the constraining system. Since $Y(\omega)$ is the driving-point admittance of a linear system, resonance and antiresonance frequencies alternate (see, for example, Skudrzyk 1980). Thus frequencies of perfect transmission and perfect reflection alternate, both occurring on average at the modal density of the constraining system alone.

The function $Y(\omega)$ may be written in terms of the eigenvalues and normal modes of the constraining system (Hodges & Woodhouse 1986)

$$Y(\omega) = -\sum_n \frac{\mathrm{i}\omega u_n^2}{\omega_n^2 - \omega^2}, \tag{2.5}$$

where $u_n$ is the $n$th mass-normalized mode shape (evaluated at the point of attachment to the string) and $\omega_n$ its frequency. This result makes it easy to investigate the width of the transmission peaks. Near the $n$th modal frequency of the constraining system, assuming low modal overlap, the admittance will be well approximated by one term from the summation of (2.5), so that

$$T \approx \frac{2\mathrm{i}\omega u_n^2}{2\mathrm{i}\omega u_n^2 - Y_0(\omega_n^2 - \omega^2)}. \tag{2.6}$$

This has the familiar form of the response of a damped single-degree-of-freedom system to forcing, so that we may write down the 'half-power bandwidth' of the perfect-transmission peak in $T(\omega)$:

$$\Delta_n \approx 2u_n^2(0)/Y_0. \tag{2.7}$$

This bandwidth has its origin in the radiation damping of the constraint mode induced by connecting it to the semi-infinite strings.

## 3. A symmetric constraint on a one-dimensional system

Much of the behaviour seen in this simple example can be generalized to a class of one-dimensional wave-bearing systems, on which an attached structure or other inhomogeneity produces some reflection of waves. The system to be considered is shown schematically in figure 1. Two semi-infinite homogeneous sections capable of supporting a single propagating wavetype are connected through an intermediate system, which may act at a point or be of finite extent in the $x$ direction. The only stipulations on this junction are that it be conservative and symmetric with respect to the transformation $x \to -x$.

For an incident wave from the left, reflection and transmission coefficients $R$ and $T$ may be defined by assuming displacement fields as shown in figure 1. From the assumption of symmetry, the same coefficients will govern reflection and transmission of a wave incident from the right. Now consider symmetric excitation of the




PHILOSOPHICAL TRANSACTIONS OF THE ROYAL SOCIETY A MATHEMATICAL, PHYSICAL & ENGINEERING SCIENCES

system, with waves of equal amplitude and phase incident from both right and left. After interaction with the junction structure, outgoing waves $(R+T)\,\mathrm{e}^{-\mathrm{i}(\omega t \pm kx)}$ will travel to the left (+ sign) and right (− sign). Evanescent waves will also be produced near the junction, decaying away from it symmetrically on both sides. Internal motions of the junction structure will be excited, but only those which are symmetric under $x \to -x$.

Under this symmetric excitation, it is plain that there is no net energy flux passing any point in the system. Considering the combined wavefield beyond the reach of the evanescent fields, it follows that $|R+T| = 1$. So let

$$R+T = \mathrm{e}^{2\mathrm{i}\theta_+}, \tag{3.1}$$

where $\theta_+$ is a function of frequency, which is well-defined mod $\pi$ and can be chosen continuous. The displacements in the wavefield, on the left say, away from the evanescent parts are then

$$\mathrm{e}^{-\mathrm{i}(\omega t - kx)} + \mathrm{e}^{2\mathrm{i}\theta_+}\,\mathrm{e}^{-\mathrm{i}(\omega t + kx)} = 2\mathrm{e}^{-\mathrm{i}(\omega t - \theta_+)}\cos(kx - \theta_+) \tag{3.2}$$

so that they are in phase everywhere.

Now choose a symmetric pair of points on the left and the right in the far wavefield, at an antinodal point of this standing wave. Formally, we can join these two points by imposing periodic boundary conditions, without in any way changing the displacement fields. The result is a finite system that satisfies the condition of phase closure at the artificially joined point. But this is one standard way of determining normal mode frequencies of a finite system (see, for example, Cremer *et al.* 1973 §II, 4). So we may deduce that all other generalized coordinates, including those describing the evanescent fields and the internal degrees of freedom of the joint structure, are also moving in the same phase. Thus we may regard $\theta_+$ as the phase of a transfer function, taking the symmetric pair of incoming waves as input and the response of one of the generalized coordinates describing the joint structure as output. But the behaviour of the phase of forced response of a resonant structure is very familiar: it increases by $\pi$ for each mode which is excited. In this case, these are the modes of the junction which are symmetric under $x \to -x$. Of course, we ignore any modes which are uncoupled to the wave motion. We also assume that the modes are non-degenerate.

This argument may be repeated for the case of an antisymmetric pair of incoming waves (equal amplitude but opposite phase in the far wavefield). Analogously to (3.1), we find

$$R-T = \mathrm{e}^{2\mathrm{i}\theta_-}, \tag{3.3}$$

say, where $\theta_-$ changes by $\pi$ each time the frequency passes through a mode of the junction structure which involves motion which is antisymmetric under $x \to -x$. Combining the two cases, we may deduce

$$\frac{R+T}{R-T} = \mathrm{e}^{2\mathrm{i}(\theta_+ - \theta_-)}. \tag{3.4}$$

from which it follows that

$$T/R = \mathrm{i}\tan(\theta_+ - \theta_-). \tag{3.5}$$

This shows that the result displayed for the string with a point attachment in (2.3) is quite general: the transmitted and reflected waves are in quadrature for any system satisfying the symmetry conditions assumed here.

It also follows immediately from (3.5) that whenever $(\theta_+ - \theta_-) = n\pi$, $T = 0$ and there is perfect reflection of waves from the junction. Conversely, whenever $(\theta_+ - \theta_-) = (n + \frac{1}{2})\pi$, $R = 0$ and there is perfect transmission through the junction. Combining these results with the earlier remarks about the frequency dependence of $\theta_+$ and $\theta_-$ yields a direct link between the resonances of the junction structure and the number and distribution of frequencies of perfect reflection and perfect transmission. Suppose first that the junction has only symmetric resonances, so that $\theta_-$ is constant. Then $\theta_+$ is monotonically increasing, through $\pi$ for each resonance, and there is a strict alternation of frequencies of perfect reflection and perfect transmission. This is the case illustrated in §2, since a point attachment to a stretched string could only exhibit symmetric modes of vibration (as a string cannot support a point moment applied to it). Similar behaviour would occur in the converse case, in which the junction structure allowed only antisymmetric modes.

The general case is rather more complicated. The behaviour depends on $\theta_+ - \theta_-$, so that there is scope for the influences of symmetric and antisymmetric junction modes to interact. If the modes are well separated (compared with the extent by which they are broadened by radiation damping), there will be no significant interaction. The phases $\theta_+$ and $\theta_-$ each flip by $\pi$ for each resonance, so that corresponding to each resonance of the junction structure alone we may expect to find one frequency of perfect transmission and one of perfect reflection. The precise frequencies at which these occur depend on how the junction mode is influenced by coupling to the evanescent and travelling waves of the wave-bearing systems. If the modes overlap, things are less clear-cut. If there is a difference in modal densities between symmetric and antisymmetric junction modes, then whatever happens there is an inexorable trend in $\theta_+ - \theta_-$ based on the difference of the two, and that sets a minimum density of frequencies of perfect reflection and perfect transmission. But they will in general occur more frequently than this minimum, as will be illustrated by examples in the next section.

## 4. Deterministic examples

### (*a*) *Point-constrained bending beam*

The simplest system to exhibit the full range of behaviour revealed in the previous section is a bending beam (with line density $m$ and bending stiffness $B$) with a point attachment that has resonances in both transverse and torsional motion (but no coupling between the two, to satisfy the assumption of symmetry). So suppose that at the point $x = 0$, a linear system is attached which presents a transverse admittance $Y_t(\omega)$ and a rotational admittance $Y_r(\omega)$. For an incident wave from the left, assume displacement fields

$$\begin{aligned} u(x,t) &= \mathrm{e}^{-\mathrm{i}\omega t}[\mathrm{e}^{\mathrm{i}kx} + R\,\mathrm{e}^{-\mathrm{i}kx} + D\,\mathrm{e}^{kx}] \quad (x \leqslant 0), \\ u(x,t) &= \mathrm{e}^{-\mathrm{i}\omega t}[T\,\mathrm{e}^{\mathrm{i}kx} + F\,\mathrm{e}^{-kx}] \quad (x \geqslant 0), \end{aligned} \tag{4.1}$$

where $k = [m\omega^2/B]^{\frac{1}{4}}$. Imposing the four boundary conditions at $x = 0$ and solving the resulting simultaneous equations, the solution for the reflection and transmission coefficients may conveniently be written in the form

$$R + T = \frac{2(1-\mathrm{i}) - h}{2(1-\mathrm{i}) + \mathrm{i}h}, \quad R - T = -\frac{2(1+\mathrm{i}) + g}{2(1+\mathrm{i}) + \mathrm{i}g}, \tag{4.2}$$

where

$$g = -\mathrm{i}\omega/Y_r Bk, \quad h = -\mathrm{i}\omega/Y_t Bk^3. \tag{4.3}$$

In terms of the formalism of §3, this yields

$$\theta_+ = \arctan(1-\tfrac{1}{2}h)-\tfrac{1}{4}\pi, \quad \theta_- = -\arctan(1+\tfrac{1}{2}g)-\tfrac{1}{4}\pi. \tag{4.4}$$

As expected, $\theta_+$ depends only on the symmetric motion of the constraint, via the function $h$ involving the transverse response, while $\theta_-$ depends only on the antisymmetric motion via the function $g$ involving rotational response. Solving for the symmetric and antisymmetric combination of the evanescent fields yields

$$F+D = -2\sin\theta_+ \, e^{i\theta_+}, \quad F-D = 2\cos\theta_- \, e^{i\theta_-}. \tag{4.5}$$

These have the appropriate phases $\theta_+$ and $\theta_-$ respectively, as predicted by the general argument in §3.

From (4.4) it is possible to deduce the behaviour of $\theta_+$ and $\theta_-$ in various limiting cases. If the symmetric constraint is weak, then $h$ will be small at most frequencies. For a strong constraint, on the other hand, $h$ will generally be large. Similar remarks apply to the function $g$ in respect of the strength of antisymmetric constraint. The symmetric and antisymmetric constraints do not necessarily have the same order of magnitude of strength, as will be seen in §4*b*. Now it is clear that when $h = 0$, $\theta_+ = 0$, and when $h \to \infty$, $\theta_+ = \frac{1}{4}\pi$. Similarly, when $g = 0$, $\theta_- = \frac{1}{2}\pi$, and when $g \to \infty$, $\theta_- = \frac{1}{4}\pi$. (All these phases are given mod $\pi$.) So for weak or strong constraints with the respective symmetries, the corresponding phases can be expected to lie close to these limiting values at most frequencies, flipping rapidly through $\pi$ when the pattern of constraint resonances and antiresonances requires it. It follows that if both constraints are weak, then $|\theta_- - \theta_+| \approx \frac{1}{2}\pi$ and $|T| \approx 1$ at most frequencies as one would expect. Conversely if both constraints are strong, $|\theta_- - \theta_+| \approx 0$ so that $|T| \approx 0$ at most frequencies. Finally, if one constraint is weak and the other strong (an extreme case being a rigidly pinned point constraint), then $|\theta_- - \theta_+| \approx \frac{1}{4}\pi$, and $|T| \approx 1/\sqrt{2}$.

To see this behaviour in detail, it is convenient to work in terms of a specific example. Let the attached system be a finite section of another bending beam lying parallel to the infinite beam. This is assumed to be rigidly attached to the infinite beam at its centre point, and to have both ends free so that it acts as a double cantilever. The symmetric vibration modes of the finite beam will couple to the wave-bearing beam via a transverse force, and will govern the behaviour of $\theta_+$. The antisymmetric modes have a nodal point at the beam centre, but will couple via a moment and will govern $\theta_-$. The two sets of modes alternate on the unconstrained finite beam, of course. The system may be regarded as a multi-mode 'tuned absorber' attached to the infinite beam (although no damping is allowed in the system for the present purpose).

By allowing the attached beam to have different properties to those of the infinite beam, it is possible to investigate different régimes of strength of coupling. We will suppose that the finite beam has bending stiffness $\lambda B$ and line density $\lambda m$. Small values of $\lambda$ will correspond to weak constraint (for both symmetric and antisymmetric motion), while large values of $\lambda$ will correspond to strong constraint. The functions $\theta_+$ and $\theta_-$ can be readily computed, using the fact that the two admittance functions for this particular constraint system are

$$Y_t = \frac{i\omega}{2\lambda B k^3} \frac{[1+\cos kL \cosh kL]}{[\cosh kL \sin kL + \cos kL \sinh kL]} \tag{4.6}$$

and

$$Y_r = \frac{i\omega}{2\lambda B k} \frac{[1+\cos kL \cosh kL]}{[\cosh kL \sin kL - \sinh kL \cos kL]}, \tag{4.7}$$

where the attached beam is of length $2L$.

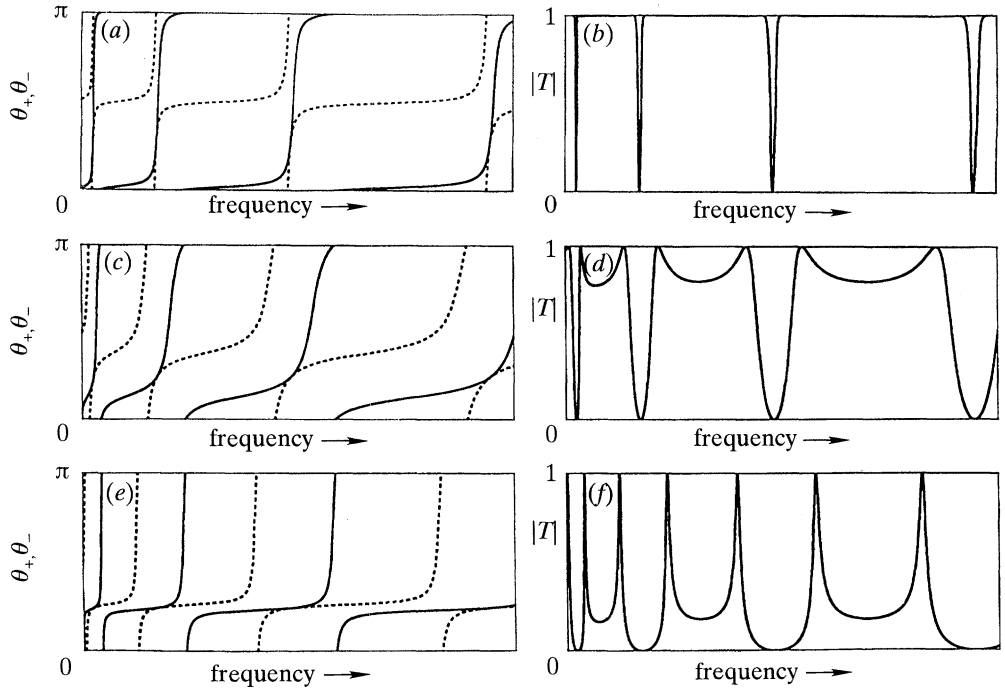


Figure 2. Phase angles $\theta_+$ and $\theta_-$ (left-hand column) and transmission coefficients (right-hand column) plotted against frequency, for a symmetric free-free beam rigidly attached at its centre to an infinite beam. The attached beam has bending stiffness and line density $\lambda$ times those of the infinite beam, where $\lambda = 0.1$ (top row), 1 (middle row) and 10 (bottom row).

Results are shown in figure 2*a*, *c*, *e*, for values $\lambda = 0.1$, 1 and 10. These illustrate the general characteristics expected from the preceding discussion. For $\lambda = 0.1$, $\theta_+$ has plateaux around the value 0, while $\theta_-$ has them around $\frac{1}{2}\pi$. Conversely for $\lambda = 10$, the plateaux lie at $\frac{1}{4}\pi$ for both phase angles. For $\lambda = 1$ intermediate behaviour is seen, with less strongly marked plateaux. A similar sequence of behaviour would be expected from any other attached constraint system, as the strength of coupling was varied. The set of $\theta_+$ curves all pass through the same values at the points where $\theta_+ = 0$ and $\frac{1}{4}\pi \pmod{\pi}$. This is because at the frequencies at which $h = 0$ or $\infty$, the multiplying factor governing the constraint strength does not matter. Similarly, the $\theta_-$ curves all pass through the same values at the frequencies where $\theta_- = \frac{1}{2}\pi$ and $\frac{1}{4}\pi$, corresponding to $g = 0$ and $\infty$.

The corresponding transmission coefficients are shown in figure 2*b*, *d*, *f*. The general discussion of §3 leaves some doubt as to exactly what will be seen in this case. The symmetric and antisymmetric resonances have the same modal density, so it is conceivable that the effects of $\theta_+$ and $\theta_-$ would cancel, and that there would be no frequencies of perfect transmission or perfect reflection. At the other extreme, when the constraint resonances are well separated we might expect to find one perfect reflection frequency and one perfect transmission frequency per mode. What is revealed by the calculation is intermediate between these two. For all cases of coupling strength it turns out that there is a perfect-transmission frequency for every constraint mode, but that perfect reflection occurs only every two modes. It occurs at the clamped-free half-beam frequencies, where $Y_r$ and $Y_t$ both vanish: these are




PHILOSOPHICAL TRANSACTIONS OF THE ROYAL SOCIETY A MATHEMATICAL, PHYSICAL & ENGINEERING SCIENCES

frequencies of perfect reflection whatever the ratio of stiffness to density for the attached beam. But the fact that the $\theta_+$ and $\theta_-$ curves just touch at those frequencies in figure 2 is specific to the case where the attached beam has the same ratio as the infinite one: for differing ratios the curves will cross, producing two frequencies of perfect reflection per pair of constraint modes.

### (*b*) *Cylindrical shell with a plane baffle*

A more complicated example of the behaviour discussed in §3, and one of direct engineering significance, is a thin, circular cylindrical shell with a thin panel bridging the interior in a plane perpendicular to the cylinder generators. It is representative of, for example, a tank with a baffle or an airframe structure with a bulkhead. At first sight it might appear that the results of §3 do not apply to this system, because it is not one dimensional. However, the cylindrical symmetry of both wave-bearing system and constraint means that any possible motion of the system can be decomposed into waveguide modes, in which radial shell motion may be assumed to vary with azimuthal angle $\phi$ according to $\cos n\phi$ or $\sin n\phi$, where $n = 0, 1, 2, 3, \ldots$, labels the successive waveguide modes. We refer to $n$ as the 'angular order' of a given waveguide mode.

For each angular order, considered separately, we have a one-dimensional problem of the kind discussed in §3. The plane baffle obviously satisfies the symmetry assumption. There are in general four wavetypes on a thin cylindrical shell, of which up to three may be propagating. However, for an angular order of 2 or greater, the two propagating wavetypes involving predominantly in-surface motion have cut-on frequencies significantly higher than that of the predominantly flexural wavetype. Thus for a range of low frequencies, the assumption of a single propagating wavetype is satisfied. There are then three evanescent wavetypes.

This is a system for which the constraint strength for symmetric and antisymmetric motion will be very different. Symmetric motion of the shell couples to the in-plane motion of the circular plate, whereas antisymmetric motion of the shell couples to flexural motion of the plate. When the plate is thin, one would anticipate that the flexural motion will present a high admittance to the shell, compared with the in-plane motion which will generally present a much lower admittance. Also, the modal densities of the symmetric and antisymmetric resonances of the constraining system will be quite different. The modal density of flexural modes in the plate will be much higher than that for the in-plane modes, provided again that the plate is thin.

Applying the result of §3 now produces a surprising prediction. Since the modal density of antisymmetric resonances is much greater than that of symmetric resonances, $\theta_+ - \theta_-$ will have a systematic trend dominated by the behaviour of $\theta_-$, and there will inevitably be a sequence of frequencies of perfect reflection and perfect transmission. But these arise from the rather low-impedance flexural modes of the baffle, and in spite of the fact that the in-plane motion imposes a strong constraint on the cylinder at almost all frequencies. One might have expected some enhancement of transmission around flexural resonances, but that the in-plane constraint can be overcome entirely to produce perfect transmission is not perhaps immediately intuitive.

Detailed computation confirms this prediction. For this purpose, the required symmetric and antisymmetric impedances of the circular plate may be inferred from the classic works of Love (1927, §314) and Rayleigh (1877, §218, *et seq.*), while the modelling of the cylinder follows Arnold & Warburton (1949). As an example, we




PHILOSOPHICAL TRANSACTIONS OF THE ROYAL SOCIETY A MATHEMATICAL, PHYSICAL & ENGINEERING SCIENCES

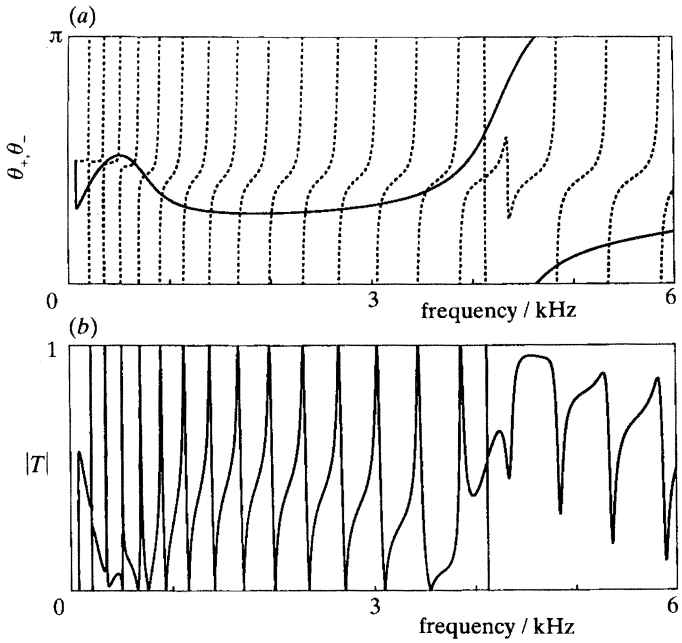


Figure 3. (*a*) Phase angles $\theta_+$ (solid) and $\theta_-$ (dashed) and (*b*) transmission coefficient plotted against frequency, for vibration with angular order $n = 4$ on an infinite thin circular cylinder with a thin, plane circular baffle (as described in the text).

consider a steel cylinder of radius 1 m and thickness 5 mm, and a steel baffle of thickness 5 mm. The ring frequency for this cylinder lies at 867 Hz. We show first some results for a typical angular order, $n = 8$. The cut-on frequencies for the three propagating wavetypes are 78 Hz (flexural waves), and 4133 Hz and 6990 Hz (in-surface waves). There is indeed a wide range of frequencies for which only flexural waves can propagate, within which the result of §3 may be applied.

The computed transmission coefficient $T(\omega)$ is plotted in figure 3*b*. Behaviour in the expected pattern is immediately apparent, with frequencies of perfect transmission and perfect reflection occurring approximately at the modal density of flexural resonances in the baffle. The cut-on frequency for flexural waves is visible at the left of figure 3*b*. The lower cut-on for in-surface motion makes itself apparent in a more subtle way. For frequencies above this, while the transmission coefficient continues to have peaks associated with flexural resonances of the baffle, those peaks no longer reach a magnitude of unity. This is to be expected, since some of the incident energy can now be scattered into the other propagating wavetype at the baffle.

The functions $\theta_+$ and $\theta_-$ are plotted in figure 3*a*. They present very different appearances, as would be expected from the discussion above. The in-surface motion has only a single resonance in the frequency range plotted, so that the $\theta_+$ curve is slowly varying. The hump at low frequencies arises from the dispersion characteristics of wave propagation on the cylinder for this angular order: on the low-frequency side of the hump the cylinder is significantly stiffened by curvature effects (relative to a flat plate of the same thickness and material) (Arnold & Warburton 1949). This effect diminishes as the ring frequency is approached, and above that the behaviour is much closer to that of a flat plate. This phenomenon also produces an effect on $\theta_-$.

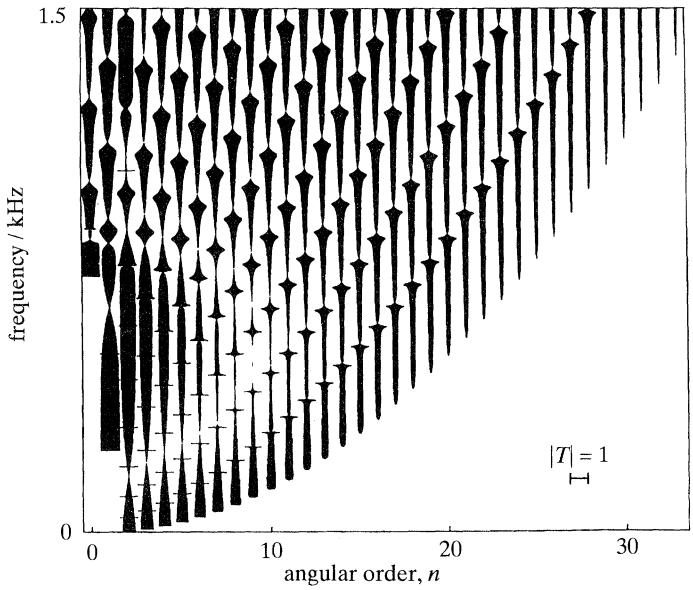


Figure 4. Transmission coefficient for the baffled cylinder problem of figure 3, plotted against frequency and angular order.

At very low frequencies, corresponding to the rise of the hump in $\theta_+$, the peaks of perfect transmission are extremely narrow since the impedance mismatch between baffle and cylinder is quite large. Once the ring frequency is approached, the radiation damping of the baffle modes by the infinite cylinder increases and the peaks become broader.

The computation may be repeated for the other angular orders. The resulting transmission coefficients for $n = 0, 1, \ldots, 33$ are all plotted in figure 4, for frequencies up to 1500 Hz. For each value of $n$, the result is represented by a vertical stripe whose width is modulated in proportion to the transmission coefficient magnitude. The stripes for $n = 0$ and 1 are truncated at low frequencies, when the associated cylinder displacement becomes predominantly in-surface rather than radial. The frequencies of perfect transmission appear as the wide spots on each stripe, and the systematic variation of these frequencies with $n$ is evident in the figure. The curves traced out by these perfect transmission frequencies can be thought of as lines along which trace wavenumber coincidence occurs between waves on the cylinder and in the baffle.

## 5. Implications for statistical energy analysis

### (a) *The effect on variance of* SEA *estimates*

Once the transmission coefficient through a junction has been calculated, the standard SEA procedure is to turn this into a coupling loss factor by various averaging processes. These include some or all of: frequency averaging over a chosen bandwidth; ensemble averaging over systems whose properties and dimensions are drawn from a statistical population representing manufacturing tolerances; and (if the junction is extended in one or two dimensions) averaging over angles of incidence of waves on the boundary, assuming a diffuse field within the source subsystem. Frequency averaging and ensemble averaging may in fact be the same process, if an

ergodic assumption is made about the effect of manufacturing differences on the subsystem frequency response functions.

For a resonant coupling of the kind investigated here, the first issue to consider is the bandwidth for frequency averaging, compared with the expected spacing of frequencies of perfect transmission. The usual SEA philosophy is to make sure that the averaging bandwidth is wide enough to contain at least a few modes of each subsystem, because the essence of SEA is to lose the unwanted detail of individual modal responses. One might therefore suppose that the same argument should be applied to the 'modes', that is the frequencies of perfect transmission, of any junctions in the system. Averaging over a very narrow band will give a coupling loss factor which has significant frequency variation (Woodhouse 1981), although if an ensemble average is also carried out this variation may be smoothed out.

But if the junction transmission coefficient is averaged over a sufficiently wide band that a smoothly-varying answer is obtained, then a trap has been concealed which may have a profound effect on the overall accuracy of the SEA model. The effect is most striking for a junction which behaves like figure 2*f*, with a transmission coefficient which is generally low except for narrow peaks at which it reaches unity. The calculated coupling loss factor will then be quite small, leading one to expect a situation with 'weak coupling', for which SEA is always said to work well (Lyon 1975; Hodges & Woodhouse 1986). But the energy transmission by such a junction is very selective: the source subsystem may have a uniform distribution of vibrational energy in frequency, but the transmitted vibration will be strongly concentrated in the narrow bands where the transmission is high.

If only these two subsystems are involved, this filtering may not matter very much. A correct SEA model should predict the mean-square level in the second subsystem accurately. The difficulty arises if this second subsystem is coupled to a third by another junction with resonant properties. Then one of two things can happen, and neither of them is handled very well by conventional SEA. If the second junction is the same as the first, the energy incident on it is 'pre-filtered' to fit its pattern of strong transmission. So one can expect a much higher proportion of the energy to be transmitted across the second junction than across the first. This leads to a phenomenon of 'diminishing returns' if the system geometry has a chain of similar couplings. Explicit analysis of this phenomenon, based on two quite different approaches, has been given by Heron (this Issue) and Langley & Bercin (this Issue).

If the second junction is different from the first, a different problem arises. Typically, the very small number of perfect-transmission peaks within a given frequency band will not line up in the two junctions, so that the field which has been filtered by the first junction will transmit less well through the second than would have been the case for a spectrally-white incident field. The normal, linearly-averaged SEA coupling loss factor is not a very good measure of this energy transmission. If the conventional coupling loss factors are used, this phenomenon will produce an increase in the variance around the SEA mean prediction, when different members of the statistical ensemble are tested. It is possible that this variance could be reduced by a different choice of averaging procedure for the coupling loss factors (Hodges & Woodhouse 1986).

Similar considerations apply to a junction which is extended in one or two dimensions. For example, the data of figure 4 can be used to calculate a coupling loss factor. As well as a frequency average, a suitable weighted sum of the results for different angular orders must be taken, to represent a diffuse field incident on the





PHILOSOPHICAL TRANSACTIONS OF THE ROYAL SOCIETY A MATHEMATICAL, PHYSICAL & ENGINEERING SCIENCES

junction (Lyon 1975 §3.3; Langley 1993). Perfect transmission occurs at different frequencies for the different values of $n$, and one does not require such a broad averaging bandwidth to achieve a smoothly varying random-incidence transmission coefficient, from which a coupling loss factor may be obtained. Filtering effects are produced by this junction too, not only filtering in frequency but also in circumferential wavenumber. This can produce similar effects to those noted for the beam example, for example diminishing returns from successive transmission through identical junctions (Langley & Bercin, this Issue).

### (*b*) *When is a junction a subsystem?*

There is a second general issue raised by junctions with internal degrees of freedom: under what circumstances does it become necessary to treat the coupling as an energy-storing subsystem in its own right? Of course, if one needs to allow for damping in the junction structure, or excitation on it, then the SEA formalism requires that it appears as a subsystem. Problems associated with low modal density may then arise, but those are familiar and are not the subject of this investigation. We consider here the question of accuracy of modelling: the example from §4*a* will be analysed as a two-subsystem problem with complicated coupling and as a three-subsystem problem with simpler coupling, and the results compared.

Consider first the general problem of two joined systems, with energies $E_1$ and $E_2$ and modal densities $n_1$ and $n_2$, having a third system attached symmetrically at the junction point. This third system is assumed to have no damping or external drive, and to have energy $E_3$ and modal density $n_3$. Suppose that the subsystems 1 and 2 are locally physically similar (for example, two sections of beam with the same cross-section but perhaps different lengths). Using the normal SEA formalism (Lyon 1975 §3.2), a requirement of power balance on the third subsystem gives

$$E_3/n_3 = \tfrac{1}{2}[E_1/n_1 + E_2/n_2] \tag{5.1}$$

(where advantage has been taken of the symmetry of coupling $1 \leftrightarrow 3$ and $2 \leftrightarrow 3$). In terms of the thermal analogy of SEA, the attached system adjusts to the mean 'temperature' of the other two subsystems. This equation may be used to eliminate $E_3$ and $n_3$ from the other two power-balance equations, and the result is an 'equivalent two-subsystem model' derived from the three-subsystem model. If the coupling factors (i.e. the products of coupling loss factor and modal density which satisfy reciprocity) in the three-subsystem model are $\epsilon_\alpha$ (between systems 1 and 2) and $\epsilon_\beta$ (between systems 1 or 2 and system 3), then the equivalent coupling factor between systems 1 and 2 in the two-subsystem model turns out to be $(\epsilon_\alpha + \frac{1}{2}\epsilon_\beta)$.

To apply this to the example of §4*a*, we first calculate the transmission coefficients for the problem in which the two halves of the attached cantilever beam are regarded as semi-infinite. These can be used to calculate the coupling factors $\epsilon_\alpha$ and $\epsilon_\beta$ by the usual SEA wave-method approach. But for the present purpose it is easier to work in reverse and deduce an equivalent transmission coefficient from the argument given above, which can be compared directly with a suitably averaged value of the transmission coefficients plotted in figure 2.

The calculation of the transmission coefficients at a junction of four semi-infinite beams is quite straightforward. The general expressions for the answers are quite lengthy, but when the assumption is made, as before, that the 'attached' beams have bending stiffness $\lambda B$ and line density $\lambda m$ (compared to the corresponding properties $B$ and $m$ of the original semi-infinite beams) they reduce to very simple expressions.

The (energy) transmission coefficient between the two sections of original beam is $\tau_1 = 1/(1+\lambda)^2$, and that from a section of original beam to a section of 'attached' beam is $\tau_2 = \lambda/(1+\lambda)^2$. Noting that the attached subsystem is composed of both (identical) sections of attached beam, the required equivalent transmission coefficient, based on $(\epsilon_\alpha + \frac{1}{2}\epsilon_\beta)$ from above, is then

$$\tau_1 + \tau_2 = 1/(1+\lambda). \tag{5.2}$$

So for the case of figure 2*f* with $\lambda = 10$, the equivalent transmission coefficient is 1/11, −10.41 dB.

When a frequency average is performed on the results plotted in figure 2*f*, choosing one 'cycle' of the obvious pattern as the bandwidth, the result rapidly converges to 0.9836, −10.07 dB. (At very low frequencies it is slightly different, largely because of the influence of the evanescent fields.) So for this example, the two methods agree with some accuracy. Numerical experiments reveal that this agreement persists over a very wide range of assumed properties of the attached beam. So at least for this idealized problem, it seems that one can treat the attached beam as a complicated coupling or as a third subsystem, and obtain essentially the same SEA model by either route. It would be interesting to test this conclusion on other combinations of wavebearing system and junction structure.

## 6. Conclusions

Resonant couplings of the kind examined here produce strong frequency dependence of the transmission coefficient, and this can have significant implications for the result and interpretation of vibration analysis, whether deterministic or statistical, of a system which includes the junction. Frequencies of perfect transmission and of perfect reflection are likely to occur, and these are a universal feature of junctions of the kind considered here. Modifications to the detailed design may move them around, but will not eliminate them unless they break the assumed symmetry. (An example of the possible usefulness of broken symmetry is the improved transmission loss when two panes of glass of different thickness are used in double glazing, compared with two identical panes.) Insight can be gained by considering the physical nature of the vibration modes of the junction. Symmetric and antisymmetric modes should be considered separately, and their modal densities and strength of coupling to the rest of the system examined.

## References

Arnold, R. N. & Warburton, G. B. 1949 Flexural vibration of the walls of thin cylindrical shells having freely supported ends. *Proc. R. Soc. Lond.* A **197**, 238–256.

Cremer, L., Heckl, M. & Ungar, E. E. 1973 *Structure-borne sound*. Berlin: Springer.

Hodges, C. H. & Woodhouse, J. 1986 Theories of noise and vibration transmission in complex structures. *Rep. Prog. Phys.* **49**, 107–170.

Langley, R. S. 1993 Elastic wave transmission coefficients and coupling loss factors for structural junctions between curved panels. *J. Sound Vib.* (In the press.)

Love, A. E. H. 1927 *A treatise on the mathematical theory of elasticity*. (Reprinted by Dover (New York) 1944.)

Lyon, R. H. 1975 *Statistical energy analysis of dynamical systems*. Cambridge, Massachusetts: MIT Press.





PHILOSOPHICAL TRANSACTIONS OF THE ROYAL SOCIETY A MATHEMATICAL, PHYSICAL & ENGINEERING SCIENCES

Rayleigh, Lord 1877 *The theory of sound*. (Reprinted by Dover (New York) 1945.)

Skudrzyk, E. 1980 The mean-value method of predicting the dynamic response of complex vibrators. *J. acoust. Soc. Am.* **67**, 1105–1135.

Woodhouse, J. 1981 An approach to the theoretical background of statistical energy analysis applied to structural vibration. *J. acoust. Soc. Am.* **69**, 1695–1709.



PHILOSOPHICAL TRANSACTIONS OF THE ROYAL SOCIETY A MATHEMATICAL, PHYSICAL & ENGINEERING SCIENCES